Medical Molecular Morphology (2019) 52:23–35
https://doi.org/10.1007/s00795-018-0199-6

ORIGINAL PAPER

Immunoreactivity patterns of tight junction proteins are useful for differential diagnosis of human salivary gland tumors

Tomoyuki Aoyama[1,2] · Akira Takasawa[1] · Masaki Murata[1] · Makoto Osanai[1] · Kenichi Takano[3] · Tadashi Hasagawa[2] · Norimasa Sawada[1]

Received: 13 March 2018 / Accepted: 18 June 2018 / Published online: 28 June 2018

Abstract
The expression pattern of tight junction proteins (TJPs) varies among organs and tumor types. In this study, we examined the immunoreactivity of claudin (CLDN)-1, -4, and -7, and JAM-A in salivary gland tumors (SGTs) by histological types and cell types to estimate their usefulness as differential diagnostic markers. Immunoreactivity of CLDN1 was higher in ductal epithelium cells of SGTs than in non-tumor tissues. Conversely, immunoreactivity of CLDN1 was significantly decreased in basal/myoepithelium cells of SGTs compared with that in non-tumor tissues. There was no significant difference between the immunoreactivity of CLDN1 in benign tumors and that in malignant tumors. Immunoreactivity of CLDN4, CLDN7, and JAM-A in ductal epithelium cells was higher in many SGTs than in non-tumor tissues. There was a difference depending on the histological type of SGT in immunoreactivity of CLDN4, CLDN7, and JAM-A in basaloid/myoepithelial cells. It was possible to classify SGTs by a hierarchical clustering using immunoreactivity of TJPs. The results suggest that an immunohistochemical marker panel including these TJPs may be useful for differential diagnosis of SGTs and that CLDN1 is associated with tumorigenesis of SGTs.

Keywords Salivary gland tumor · Tight junction · Claudin-1 · Claudin-4 · Claudin-7 · JAM-A

Introduction

Tight junctions (TJs) are intercellular junctions adjacent to the apicalmost paracellular spaces in mammalian epithelial and endothelial cells, and they regulate cell polarity and paracellular transport of ions and solutes [1, 2]. TJs consist of various combinations of claudins (CLDNs), occludin, tricellulin, and junctional adhesion molecules (JAMs). These combinations exhibit complex tissue- and cell-specific patterns of expression [3]. The CLDN family comprises crucial structural and functional components of TJs. In mammals, the CLDN family consists of 27 members. The JAM family is one of the families of proteins in the immunoglobulin superfamily. JAM-A is involved in the barrier function of TJs in epithelial and endothelial cells, and plays a role in regulation of leukocyte transendothelial migration and angiogenesis [4].

TJs also play a role in the control of homeostasis involving cell growth, differentiation, and apoptosis via various signal transduction [5]. The tissue- and cell-specific expression pattern of TJ proteins (TJPs) determines these functions. Dysfunction of TJs is closely associated with many diseases [6]. Carcinogenesis is accompanied by the disruption or loss of functional TJs. Aberrant expression and abnormal localization of TJPs have been reported in various carcinomas, and unique CLDN composition is characteristic of various cancerous tissues [6, 7]. It has been shown that expression patterns of CLDN1, 4, and 7 are altered in various carcinomas [6]. TJPs such as CLDN3, CLDN4, and JAM-A are considered to be promising targets for molecularly targeted therapy [8–11]. Clostridium perfringens enterotoxin (CPE) triggers cell death by binding to the second extracellular

Tomoyuki Aoyama and Akira Takasawa have contributed equally to this work.

✉ Masaki Murata
mmurata@sapmed.ac.jp

[1] Department of Pathology, Sapporo Medical University School of Medicine, S1. W17, Sapporo 060-8556, Japan

[2] Department of Surgical Pathology, Sapporo Medical University School of Medicine, Sapporo, Japan

[3] Department of Otolaryngology, Sapporo Medical University School of Medicine, Sapporo, Japan

loop of CLDN3 and CLDN4 [12, 13]. Xenograft tumors, including pancreas, breast, ovarian, uterine, and prostate cancers, in immunocompromised mice can be treated with CPE [14–18]. Examining the expression pattern of TJPs for each histological type of various tumors is important for the development of future molecularly targeted therapies.

Salivary gland tumors (SGTs) are relatively rare with an incidence of about 2.5–3 people per 100,000 people a year [19]. The parotid glands are the most popular as the primary lesion, in addition to the submandibular glands, sublingual glands, and also the minor salivary glands. About 70–80% of SGTs are benign tumors. Pleomorphic adenoma is the most common benign tumor and mucoepidermoid carcinoma is the most common malignant tumor. Malignant SGTs are often asymptomatic and are not diagnosed or treated until they reach an advanced stage. SGTs have very diverse and frequently overlapping histological types such as one-cell-type tumors (myoepithelioma, mucoepidermoid carcinoma, etc.) and more-than-one-cell-type tumors (pleomorphic adenoma, Warthin tumor, etc.). Moreover, many metaplastic changes (clear cell metaplasia, squamous metaplasia, oncocytic change, etc.) can occur in most of the tumor types. Although the early diagnosis and treatment are important for reducing the rate of mortality from malignant SGTs, these various histological findings also make the early diagnosis difficult.

In salivary glands, TJs provide a barrier between the extracellular environment and the glandular lumen that is critical for normal acini functions, including the maintenance of cell polarity and normal paracellular transportation of ions and solutes [20, 21]. There have been several reports on the expression of TJPs in non-tumorous salivary gland tissues such as those in patients with Sjögren's syndrome [22–28]. CLDN1, 2, 3, 4, and 16, occludin, and JAM-A are expressed in human major salivary glands, and CLDN1, 3, 4, 7, and 11 are expressed in human minor salivary glands. However, there have been very few studies on the expression of TJPs in SGTs, and immunohistological characteristics of each histological type or each cell type have not been elucidated [29, 30]. In this study, we focused on CLDN1, 4, and 7 and JAM-A expression, because these proteins are frequently expressed in a monolayer epithelium and the expression patterns of these proteins are altered in various carcinomas. The expression of TJPs (CLDN1, 4, and 7 and JAM-A) in SGTs was examined immunohistochemically, and the expression and localization of the TJPs in non-tumor tissues and various tumor tissues according to histological types and cell types were clarified.

Materials and methods

Case selection of surgical specimens

Specimens of 77 cases of SGTs obtained by surgical resections during the period from 2005 to 2014 were retrieved from the pathology file of Sapporo Medical University Hospital, Sapporo, Japan. Written informed consent was obtained from all patients for pathological assessment of their specimens, and the ethics committee of Sapporo Medical University School of Medicine approved the present study (Approval number: #282–244). Patient characteristics and clinicopathological characteristics are summarized in Table 1. The study population of 77 patients included 36 male and 41 female patients with ages ranging from 20 to 82 years. The median age of the patients was 60.5 years. The anatomical locations of the tumors were parotid gland in 60 patients, submandibular site in 13 patients, salivary gland in 13 patients, accessory parotid gland in 1 patient, and parapharyngeal space in 1 patient. The SGT specimens included 21 cases of pleomorphic adenoma (PA), 4 cases of myoepithelioma (Mye), 8 cases of basal cell adenoma (BCA), 21 cases of Warthin tumor (WT), 9 cases of mucoepidermoid carcinoma (MEC), 4 cases of adenoid cystic carcinoma (AdCC), 1 case of epithelial myoepithelial carcinoma (EMyC), 6 cases of salivary duct carcinoma (SDC), and 3 cases of myoepithelial carcinoma (MyC). EMyC, SDC, and Myc include carcinoma ex pleomorphic adenoma. As controls, adjacent interlobular ducts of non-neoplastic regions in some of the PAs and WTs were examined as non-tumor "Non-T" ($n = 40$). Since some histological change may be seen in the tissue adjacent to a tumor, we chose areas not adjacent to the tumor and areas without inflammation as non-tumor areas. The histological type was based on the WHO classification of head and neck tumors (4th edition) [19]. All slides were independently evaluated by two pathologists (TA and MM). Discordant cases were discussed, and a consensus was reached. Informed consent was obtained from all patients.

Immunohistochemical staging of surgical specimens

The H&E slides of all cases were reviewed. To exclude the possibility of histological heterogeneity of SGTs, we selected representative sections that exhibit typical histological findings. New sections from paraffin blocks were examined by the labeled polymer method using the Dako REAL™ EnVision™ Detection System (Dako ChemMate, Glostrup, Denmark) and diaminobenzidine (Dako Laboratories, Carpentaria, CA, USA) as a chromogen according

Table 1 Clinicopathological features of salivary gland tumors

Histological type	Number of cases	Age median (range)	Sex		Location of mass	
			Male	Female		
Non-tumor[a] (Non-T)	40	60.5 (20–82)	21	19	Parapharyngeal space	1
					Parotid gland	33
					Submandibular	6
Pleomorphic adenoma (PA)	21	50.4 (20–82)	9	12	Parapharyngeal space	1
					Parotid gland	13
					Submandibular	7
Myoepithelioma (Mye)	4	50.5 (27–72)	0	4	Accessory parotid gland	1
					Parotid gland	3
Basal cell adenoma (BCA)	8	62.0 (43–77)	2	6	Parotid gland	8
Warthin tumor (WT)	21	62.0 (45–79)	13	8	Parotid gland	21
Mucoepidermoid carcinoma (MEC)	9	65.0 (45–79)	1	8	Parotid gland	6
					Submandibular	3
Adenoid cystic carcinoma (AdCC)	4	57.5 (36–73)	3	1	Parotid gland	2
					Submandibular	2
Epithelial myoepithelial carcinoma[b] (EMyC)	1	59	0	1	Parotid gland	1
Salivary duct carcinoma[b] (SDC)	6	58.5 (55–77)	6	0	Parotid gland	4
					Submandibular	2
Myoepithelial carcinoma[b] (MyC)	3	48.0 (34–48)	2	1	Parotid gland	2
					Submandibular	1

[a]The interlobular ducts in non-neoplastic regions of Pleomorphic adenoma and Warthin tumor

[b]Including carcinoma ex pleomorphic adenoma

to the manufacturer's instructions. Sections were dewaxed, rehydrated, and moistened with phosphate-buttered saline (PBS) (pH 7.4), and then pretreated in an autoclave at 121 °C for 5 min in 10 mmol/l citrate buffer (pH 6.0), followed by 30-min incubation with antibodies to the following antigens in an automated immunostaining system (Dako Autostainer; Dako, Carpinteria, California, USA): CLDN-1 (Invitrogen, No.51-9000, ×100), CLDN-4 (Invitrogen, No.32-9400 × 100), CLDN-7 (IBL, No.18875, × 100), and JAM-A (Abcam, No. ab52647, × 200). We stained all 77 cases at the same time for each antibody. For evaluation of localization (immunopositive areas in the cells), we used the categories cytoplasm (C), cell membrane (M), and only TJ areas (TJ). When positive staining in two or more areas was observed, we assessed the area of strongest intensity as the main localization for statistical analysis. The intensity of staining was assessed as strong (3; c.f. Fig. 1, CLDN7 In ductal epithelium cells of Non-T), moderate (2; c.f. Fig. 1, CLDN4 In ductal epithelium cells of Non-T), weak (1; c.f. Fig. 1, JAM-A In basal/myoepithelium cells of EMyC) or negative (0; c.f. Fig. 1, and CLDN4 In basal/myoepithelium cells of PA). The proportions of positively stained tumor cells were recorded as 0 (no staining), 1 (1–10%), 2 (11–50%), 3 (51–80%), and 4 (81–100%). Since neoplasm heterogeneity caused various immunoreactivities in the cases, we used an immunoreactive score (IRS) (i.e., intensity 3 × proportion 4 = immunoreactive score 12, scale of 0–12) for improvement in accuracy [31, 32]. This method is semiquantitative.

Histologically, a salivary gland basically comprises ducts and acini. Ducts in salivary gland were divided into intercalated ducts, striated ducts, and interlobular ducts. These ducts consist of three types of cells: ductal epithelium, myoepithelial, and basal cells. Ductal epithelium cells are present at the luminal side of the duct structure. In contrast, myoepithelial and basal cells are located on the basement membrane side surrounding the luminal cells. Therefore, we evaluated the CLDNs and JAM-A immunoreactivities of SGT cells as ductal epithelium cells and basal/myoepithelium cells separately. We used p63 for marker of basal/myoepithelium cells (data not shown). To visualize the relationship between expression pattern of TJPs and cell types, we performed an agglomerative hierarchical clustering using IRS and localization of each of the CLDNs and JAM-A.

Statistics

The IRSs were compared among the groups by the Kruskal–Wallis test, followed by the Wilcoxon analyses for comparisons of their groups. p values were corrected for multiple comparisons using the Bonferroni method when appropriate. The levels of statistical significance were set at $p < 0.05$, $p < 0.01$, and $p < 0.001$. All statistical analyses were carried out using the statistical software 'EZR' (Easy R) (Division

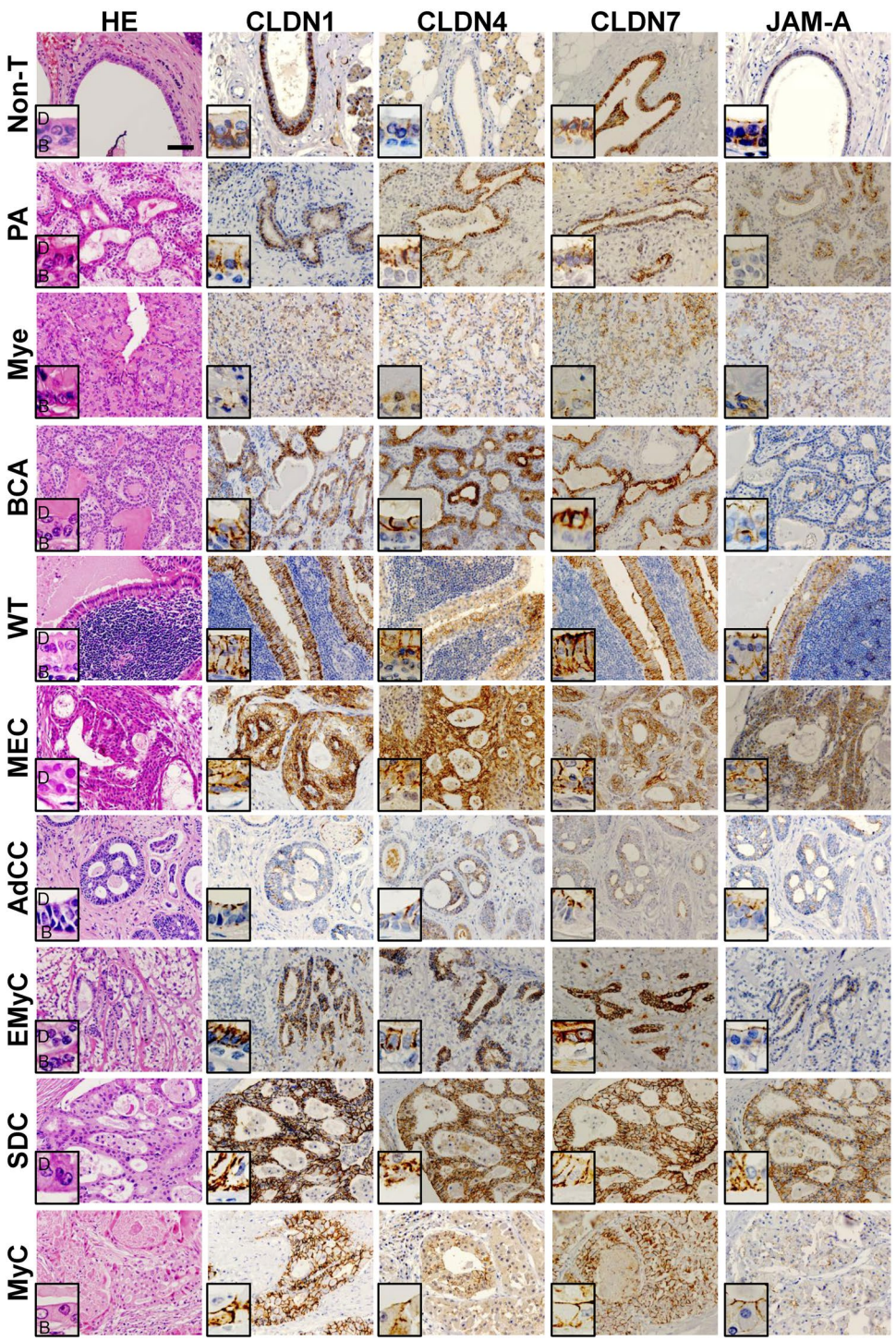

Fig. 1 Immunohistochemistry of human salivary gland samples. Paraffin-embedded sections of human tissue samples were subjected to immunohistochemical staining for CLDN1, CLDN4, CLDN7, and JAM-A, as well as hematoxylin and eosin (HE) staining. Sections were observed under a light microscope, and representative images are shown here. Bar: 100 μm. The inset in the lower left is a higher magnified view. *D* ductal epithelium cells, *B* basal/myoepithelium cells

of Hematology, Saitama Medical Center, Jichi Medical University, Saitama, Japan). Agglomerative hierarchical clustering was performed using BellCurve for Excel (Social Survey Research Information Co., Ltd., Tokyo, Japan). Euclidean distance was selected as a measure of dissimilarity and the Ward's method was used for cluster definition. A heat map was displayed using Microsoft Excel 2013.

Results

Expression patterns of TJPs according to histological types of SGTs

Representative images of immunohistochemical staining for TJPs in each histological type are shown in Fig. 1. Immunoreactivity of each TJP was assessed by the IRS. The average

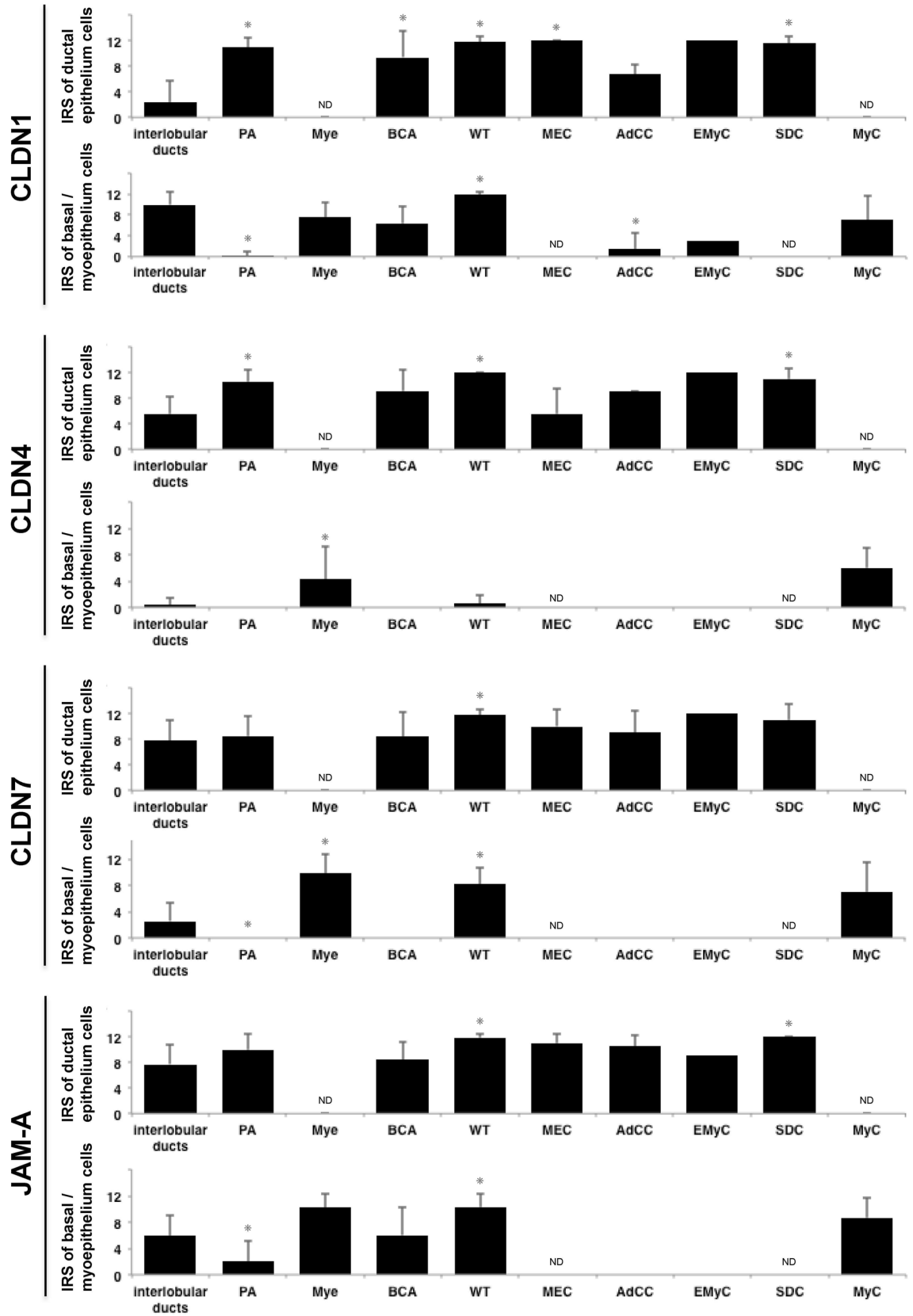

Fig. 2 IRS of TJPs in human salivary gland samples. Immunoreactivity was assessed by an immunoreactive score (IRS) (0–12), which was calculated as the product of intensity (0–3) and proportion (0–4). *$p < 0.05$

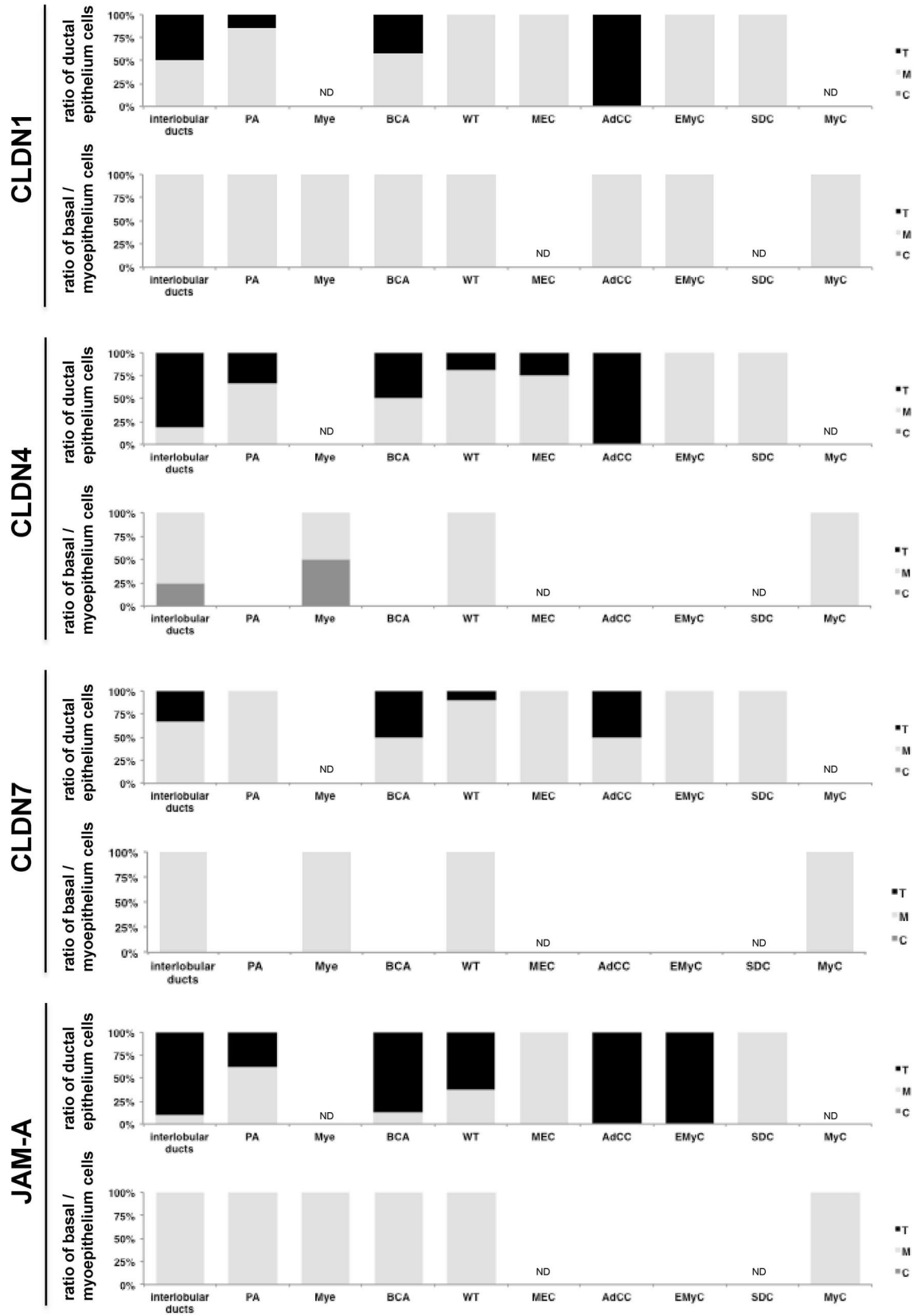

Fig. 3 Localization of TJPs in human salivary gland samples. Assessments of localization (immunopositive areas in the cells) were divided into cytoplasm (C), cell membrane (M), and only TJ areas (TJ). The ratio of the localization of TJPs in each histological type is shown in the graph. *$p < 0.001$

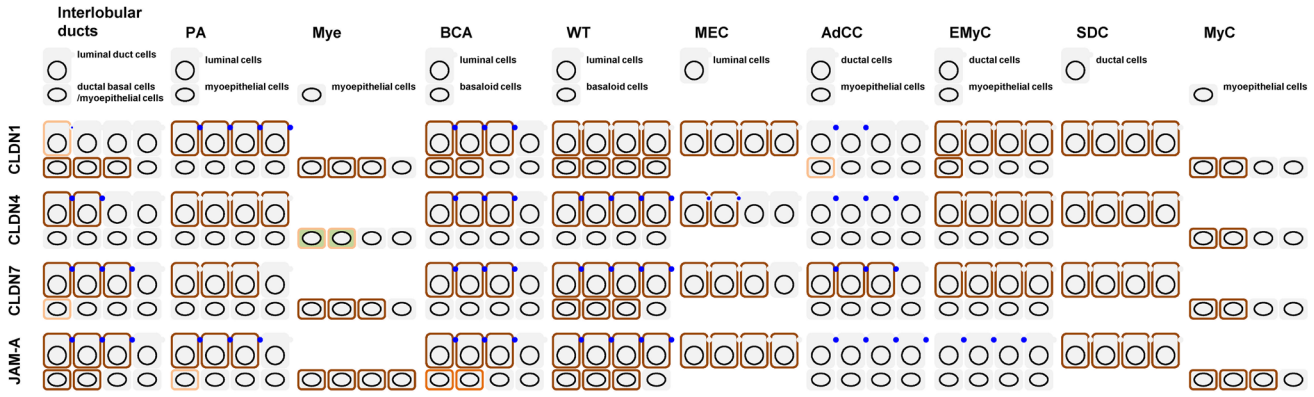

Fig. 4 Schema of subcellular localizations of TJPs in salivary gland tumors. Schematic distribution of CLDN1, 4, and 7 and JAM-A by histological types of salivary gland tumors. Blue dots and brown lines correspond to localization at TJs and basolateral cell membranes, respectively. The cytoplasm was expressed by painting with green. The intensity of staining is indicated by brightness of color or size of dot. The proportions of positively stained tumor cells are indicated by the number of colored cells: 0 (no staining), 1 (1–10%), 2 (11–50%), 3 (51–80%), and 4 (81–100%)

IRSs are shown in Fig. 2. The ratio of the localization of TJPs is shown in Fig. 3. In Fig. 4, the expression patterns of TJPs according to histological types of human SGTs are shown as a schema summarizing the above results.

CLDN1

In ductal epithelium cells, IRS of SGTs was higher than that of Non-T. Statistically significant differences were seen in IRS of SGTs except for AdCC and EMyC. In Non-T, CLDN1 localized similarly in TJ areas and in the cell membrane. In PA, WT, MEC, EMyC, and SDC, CLDN1 localized mainly in the cell membrane. In AdCC, CLDN1 localized only in the TJ areas.

In basaloid/myoepithelial cells, IRS of WT was significantly increased. IRS of PA and AdCC was significantly decreased and IRS of the other SGTs tended to be decrease. CLDN1 localized in the cell membrane in non-T and all SGTs.

CLDN4

In ductal epithelium cells, IRS of SGTs was higher than that of Non-T. Statistically significant differences were seen in IRS of PA, WT, and SDC. In Non-T and AdCC, CLDN4 localized in TJ areas. In BCA, CLDN4 localized similarly in TJ areas and in the cell membrane. In the other SDTs, CLDN4 localized mainly in the cell membrane.

In basaloid/myoepithelial cells, IRS of Mye and MyC was significantly increased. IRS was low in Non-T and WT. No expression was seen in BCA, AdCC, and EMyC. CLDN4 localized mainly in the cell membrane in non-T and SGTs. In Mye, CLDN4 also localized in the cytoplasm.

CLDN7

In ductal epithelium cells, IRS of SGTs was higher than that of Non-T. A statistically significant difference was seen in IRS of WT. In Non-T, BCA, and AdCC, CLDN7 localized in TJ areas and the cell membrane. In the other SDTs, CLDN7 localized mainly in cell membrane.

In basaloid/myoepithelial cells, IRS of Mye, WT, and MyC was higher than that of Non-T. A statistically significant difference was seen in IRS of Mye and WT. No expression was seen in BCA, AdCC, and EMyC. CLDN7 localized in the cell membrane in non-T, Mye, WT, and MyC.

JAM-A

In ductal epithelium cells, IRS of SGTs was higher than that of Non-T. A statistically significant difference was seen in IRS of WT and SDC. In Non-T, BCA, AdCC, and EMyC, JAM-A localized mainly in TJ areas. In PA and WT, JAM-A localized in TJ areas and in the cell membrane. In MEC and SDC, JAM-A localized in the cell membrane.

In basaloid/myoepithelial cells, IRS of Mye, WT, and MyC was higher than that of Non-T. A statistically significant difference was seen in IRS of WT. IRS of PA was significantly decreased. No expression was seen in AdCC and EMyC. JAM-A localized in the cell membrane.

Hierarchical clustering using IRS and localization of TJPs

When considering the above results by cell types, similarity was observed in the expression pattern of TJPs in terms of IRS and localization. We, therefore, performed cluster analysis of IRS and localization using a hierarchic agglomerative

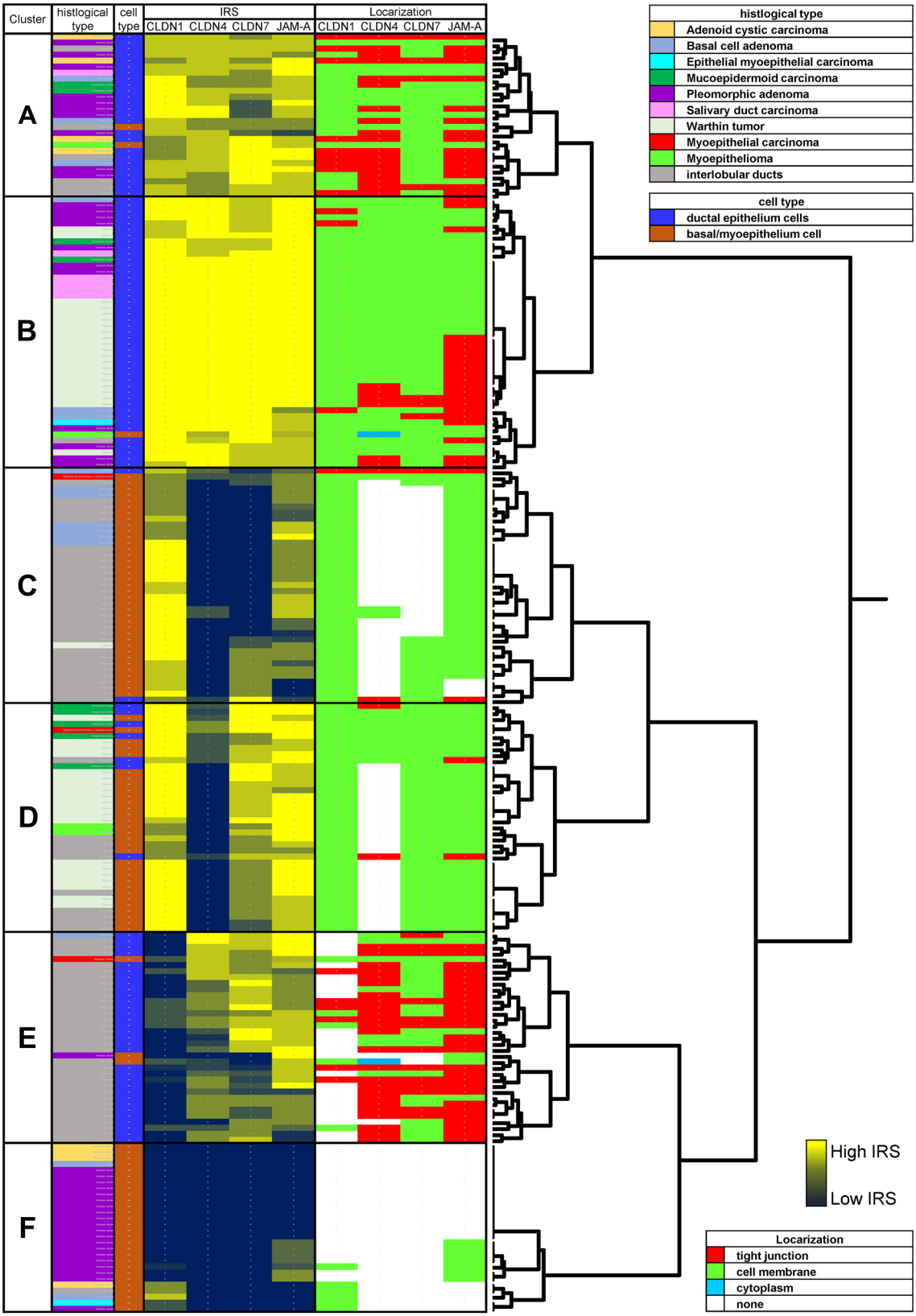
Cluster
histlogical type
cell type
IRS
CLDN1 CLDN4 CLDN7 JAM-A
Localization
CLDN1 CLDN4 CLDN7 JAM-A
A
B
C
D
E
F
histlogical type
Adenoid cystic carcinoma
Basal cell adenoma
Epithelial myoepithelial carcinoma
Mucoepidermoid carcinoma
Pleomorphic adenoma
Salivary duct carcinoma
Warthin tumor
Myoepithelial carcinoma
Myoepithelioma
interlobular ducts
cell type
ductal epithelium cells
basal/myoepithelium cell
High IRS
Low IRS
Locarization
tight junction
cell membrane
cytoplasm
none

◂**Fig. 5** Hierarchical clustering using IRS and localization of TJPs. Hierarchical clustering of salivary gland tumors and interlobular ducts using IRS and localization of each of the CLDNs (1, 4, and 7) and JAM-A. Localization of TJPs is shown on the left side of the dendrogram. Localization is indicated by only TJ areas (red), cell membrane (light green), cytoplasm (light blue), and not detected (white). IRSs of TJPs are shown by a heat map on the left side of the localization. Each colored square in the heat map represents the relative mean transcript abundance for each sample, with highest expression shown in yellow and lowest expression shown in dark blue. Histological types and cell types are shown on the left side of the heat map

method. We used Ward's method for dendrogram classification with squared Euclidean distance measures. Six different clusters formed by Non-T and SGTs, which we named clusters A–F, were obtained from this cluster analysis (Fig. 5). Almost all of the SGT cells could be distinguished from Non-T by hierarchical clustering (Fig. 5; Table 2).

The ductal epithelium cells of Non-T were mainly clustered in cluster E (31/40). Cluster E was found to have moderate IRS of CLDN7 and JAM-A and low IRS of CLDN1 and CLDN4. The ductal epithelium cells of SGTs were mainly clustered in clusters A (20/70) and B (43/70). Cluster A was found to have high/moderate IRS of TJPs. Cluster A consisted of ductal epithelium cells of AdCC (4/4), BCA (3/8), and PA (10/21). Cluster B was found to have high IRS of TJPs. Cluster B consisted of ductal epithelium cells of BCA (3/8), EMyC (1/1), PA (11/21), SDC (5/6), and WT (21/21).

The basal/myoepithelium cells of Non-T (29/40) were mainly clustered in cluster C. The basal/myoepithelium cells of BCA (6/8) were also clustered in cluster C. Cluster C was found to have high/moderate IRS of CLDN1, moderate IRS of JAM-A, and low IRS of CLDN4 and CLDN7. The basal/myoepithelium cells of SGTs were mainly clustered in clusters D (23/62) and F (27/62). Cluster D was found to have high IRS of CLDN7 and JAM-A, high/moderate IRS of CLDN1, and low IRS of CLDN4. Cluster D consisted of ductal epithelium cells of Mye (2/4) and WT (20/21). Being unusual for ductal epithelium cells, the ductal epithelium cells of MEC (5/9) was clustered in cluster D. Cluster F was found to have low IRS of TJPs. Cluster F consisted of ductal epithelium cells of AdCC (4/4), EMyC (1/1), and PA (20/21).

Comparison of IRSs in benign tumors and malignant tumors

We compared the IRS of TJPs in benign tumors (PA, Mye, BCA, and WT) and malignant tumors (MEC, AdCC, EMyC, SDC, and MyC) (Fig. 6).

Although IRS of CLDN1 was increased in ductal/epithelial cells of tumors compared with that in Non-T, there was no significant difference between benign tumors and malignant tumors. IRS of CLDN1 was significantly decreased in basal/myoepithelium cells of tumors compared with that in Non-T. Although there was no significant difference between benign tumors and malignant tumors, IRS of CLDN1 tended to be decreased.

IRS of CLDN4 was increased in ductal/epithelial cells of benign tumors compared with that in Non-T. In malignant tumors, IRS of CLDN4 was decreased compared with that in benign tumors.

There was no significant difference in the IRS of CLDN7 and that of JAM-A.

Discussion

Alteration in the expression of TJPs and mislocalization of TJPs were observed in the SGTs. Almost all of the SGT cells (clusters A, B, D, and F) could be distinguished from Non-T cells (clusters C and E) by the expression pattern of TJPs by agglomerative hierarchical clustering. Ductal epithelium cells (clusters A, B, and E) could also be distinguished from basal/myoepithelium cells (clusters C, D, and F). For ductal epithelium cells, Non-T was classified as the low IRS cluster (cluster E) and SGTs were classified as middle and high IRS clusters (cluster A and B). On the other hand, for basal/myoepithelium cells, Non-T was classified as the middle IRS cluster (cluster C) and SGTs were classified as high and low IRS clusters (cluster D and F). For localization of TJPs in ductal epithelium cells, TJPs were mostly localized in TJ areas in Non-T. On the other hand, TJPs were mostly localized in the cell membrane in SDTs. Our results suggested that the expression of TJPs has a relationship with tumorigenesis of SGTs and that an immunohistochemical panel of TJPs may be a useful diagnostic marker of SDTs. No previous study has shown classification of SGTs using the expression pattern of TJPs. Our results provide information that will become the basis of TJP study of SGTs in the future.

From the results shown in Fig. 6, it is thought that CLDN1 is strongly involved in tumorigenesis of SGTs. It was reported that CLDN1 is associated with tumorigenesis and carcinogenesis in various organs including the stomach, colon, breast, liver, lung, and thyroid [33–47]. The altered expression of CLDN1 plays different roles in a tissue-specific manner, such as regulating anoikis, induction of EMT and suppression/inhibition of cell migration, invasion, and metastasis. In our study, in ductal epithelium cells, the IRS of CLDN1 was increased in SDTs compared with that in Non-T. On the other hand, in basal/myoepithelium cells, the IRS of CLDN1 was decreased in SGTs compared with that in Non-T. The results suggested that CLDN1 may play different roles depending on the cell type in SGTs. To clarify the role of CLDN1 in SGTs, further in vitro investigation is necessary.

Table 2 Number of histological types in each cluster

	Cluster						Total
	A	B	C	D	E	F	
Ductal epithelium cells							
Adenoid cystic carcinoma	4	0	0	0	0	0	4
Basal cell adenoma	3	3	1	0	1	0	8
Epithelial myoepithelial carcinoma	0	1	0	0	0	0	1
Mucoepidermoid carcinoma	2	2	0	5	0	0	9
Pleomorphic adenoma	10	11	0	0	0	0	21
Salivary duct carcinoma	1	5	0	0	0	0	6
Warthin tumor	0	21	0	0	0	0	21
Tumor	20	43	1	5	1	0	21
Non-tumor	5	1	1	2	31	0	40
Basal/myoepithelium cells							
Adenoid cyctic carcinoma	0	0	0	0	0	4	4
Basal cell adenoma	0	0	6	0	0	2	8
Epithelial myoepithelial carcinoma	0	0	0	0	0	1	1
Myoepithelial carcinoma	0	0	1	1	1	0	3
Myoepithelioma	1	1	0	2	0	0	4
Pleomorphic adenoma	0	0	0	0	1	20	21
Warthin tumor	0	0	1	20	0	0	21
Tumor	1	1	8	23	2	27	21
Non-tumor	1	0	29	8	1	1	40
Total	27	45	39	38	35	28	

Expression of TJPs tended to be increased in ductal epithelium cells of tumors compared to that of Non-T. The increased expression levels of TJPs such as CLDN4 and JAM-A in the apical sides of tumor cells are thought to be promising targets for molecularly targeted therapy [8–11, 47, 48]. CLDN4 expression was increased in ductal epithelium cells of tumors except MEC. CLDN4 expression in MEC was the same as that in Non-T as was previously reported [29]. Immunostaining of CLDN4 was observed mainly on the cell membranes in tumors except for AdCC, whereas it was mainly observed at the TJ area in Non-T. Although CPE induced cytotoxicity in cancer cells immunolocalized with CLDN4 on the cell membranes, CPE-mediated cytotoxicity was barely detected in normal epithelial cells immunolocalized with CLDN4 in TJ areas [18]. Therefore, targeted therapy using CPE might be effective for SGTs. JAM-A is also highly expressed in ductal epithelium cells of tumors. JAM-A might, therefore, become a target of antibody therapy for malignant SGTs. CLDN4 expression was increased in ductal epithelium cells of all tumors in this study. It was previously reported that staining for CLDN1 was weak in MEC except for areas of epidermoid differentiation in low-grade MEC compared with that in normal salivary glands [29]. However, it was found in that study that CLDN1 was stained weakly at the luminal side of Non-T as was observed in the present study. When comparing on the luminal side only, CLDN1 expression is increased in MEC.

Expression of TJPs tended to be dispersed in basal/myoepithelium cells according to histological types. In PA, BCA, AdCC, and EMyC, expression of CLDN4 and CLDN7 was not observed in basal/myoepithelium cells. In addition, expression of JAM-A was not observed in AdCC and EMyC. Although expression levels of TJPs tended to be low in basal/myoepithelium cells of these tumors, high immunoreactivity of CLDN1, CLDN7, and JAM-A was observed in WT, Mye, and Myc. This expression pattern of basal/myoepithelium cells is the same as that of ductal epithelium cells of MEC and SDC. To understand this similarity, it is important to further examine each cell type individually. Expression of CLDN4 was increased compared to that of Non-T in one-cell-type tumors regardless of cell type. Targeted therapy for CLDN4 might also be effective for these tumors.

It has been reported that gene levels and protein expression of CLDN4 were shown to be higher in the order of normal salivary gland tissue, benign SGTs (PA and WT) and malignant SGTs (MEC and AdCC) by real-time PCR and immunohistochemistry [30]. In the present study, IRS of CLDN4 in non-tumor areas was lower than that in benign tumors. The immunoreactivity for CLDN4 might be different, because the antibody used in that study was different from that used in the present study. In addition, although we used interlobular ducts as non-tumor tissues, ductal and acinar cells were evaluated as control in that study. Therefore,

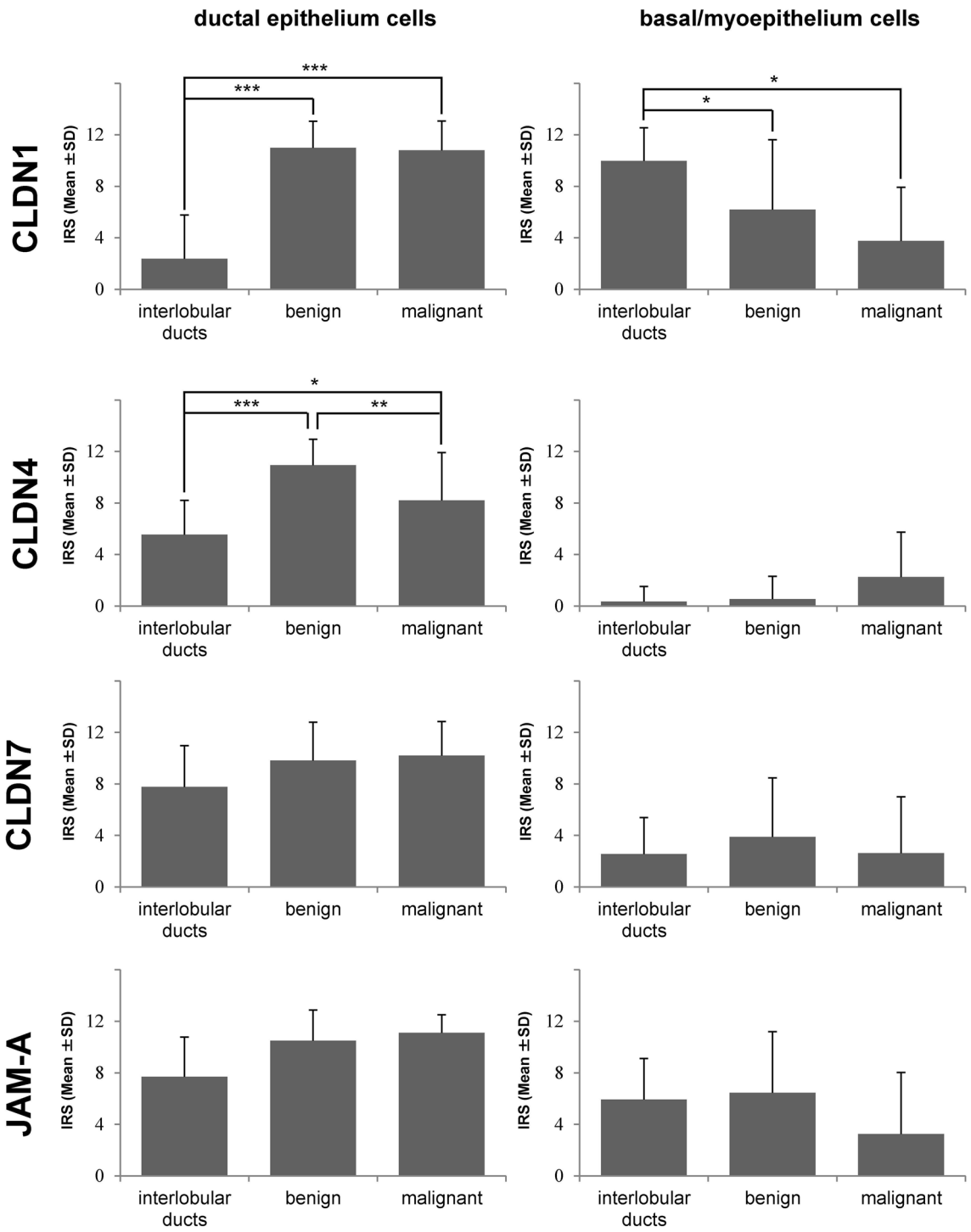

Fig. 6 Comparison of IRSs in between benign tumors and malignant tumors. Comparison of IRSs of TJPs in interlobular ducts, benign tumors (PA, Mye, BCA, and WT), and malignant tumors (MEC, AdCC, EMyC, SDC, and MyC). *$p < 0.05$, **$p < 0.01$, ***$p < 0.001$

the evaluation of CLDN4 in non-tumor tissues might be different from that in the present study.

There was difference between the localization of TJPs in non-tumor cells and that in tumor cells. Immunostaining of TJPs was commonly observed at TJ areas in non-tumor cells. On the other hand, immunostaining of TJPs was observed at cell membranes in many cases of human SGTs. TJPs, including CLDNs, have many functions as signaling molecules in cell physiology and pathology [7]. Mislocalization of these molecules may cause some dysfunction in cells.

Although there have been many reports about the expression levels of TJPs in human carcinoma tissues, there have been only a few reports about mislocalization of TJPs in human carcinoma tissues [7, 37, 47, 49, 50]. Clarification of the relationship between the mislocalization of TJPs and dysfunction in tumor cells is important for understanding the nature of the tumors.

Acknowledgements This work was supported by the Japan Society for the Promotion of Science KAKENHI Grant numbers JP16K08693 (Norimasa Sawada), JP17K08698 (Akira Takasawa), and JP16K21250 (Tomoyuki Aoyama).

Compliance with ethical standards

Conflict of interest The authors declare that they have no conflicts of interest.

References

1. Anderson JM, Cereijido M (2001) Tight junctions, 2nd edn. CRC Press, Boca Raton, pp 1–18
2. Tsukita S, Furuse M, Itoh M (2001) Multifunctional strands in tight junctions. Nat Rev Mol Cell Biol 2:285–293
3. Chiba H, Osanai M, Murata M, Kojima T, Sawada N (2008) Transmembrane proteins of tight junctions. Biochim Biophys Acta 1778:588–600
4. Severson EA, Parkos C (2009) Structural determinants of junctional adhesion molecule A (JAM-A) function and mechanisms of intracellular signaling. Curr Opin Cell Biol 21:701–707
5. Takano K, Kojima T, Sawada N, Himi T (2014) Role of tight junctions in signal transduction: an update. EXCLI J 13:1145–1162
6. Sawada N (2013) Tight junction-related human diseases. Pathol Int 63:1–12
7. Osanai M, Takasawa A, Murata M, Sawada N (2017) Claudins in cancer: bench to bedside. Pflugers Arch 469:55–67
8. Katahira J, Inoue N, Horiguchi Y, Matsuda M, Sugimoto N (1997) Molecular cloning and functional characterization of the receptor for Clostridium perfringens enterotoxin. J Cell Biol 136:1239–1247
9. Smedley JG III, Uzal FA, McClane BA (2007) Identification of a prepore large-complex stage in the mechanism of action of Clostridium perfringens enterotoxin. Infect Immun 75:2381–2390
10. Michl P, Buchholz M, Rolke M, Kunsch S, Löhr M, McClane B, Tsukita S, Leder G, Adler G, Gress TM (2001) Claudin-4: a new target for pancreatic cancer treatment using Clostridium perfringens enterotoxin. Gastroenterology 121:678–684
11. Kominsky SL, Vali M, Korz D, Gabig TG, Weitzman SA, Argani P, Sukumar S (2004) Clostridium perfringens enterotoxin elicits rapid and specific cytolysis of breast carcinoma cells mediated through tight junction proteins claudin 3 and 4. Am J Pathol 164:1627–1633
12. Santin AD, Cané S, Bellone S, Palmieri M, Siegel ER, Thomas M, Roman JJ, Burnett A, Cannon MJ, Pecorelli S (2005) Treatment of chemotherapy-resistant human ovarian cancer xenografts in C.B-17/SCID mice by intraperitoneal administration of Clostridium perfringens enterotoxin. Cancer Res 65:4334–4342
13. Santin AD, Bellone S, Siegel ER, McKenney JK, Thomas M, Roman JJ, Burnett A, Tognon G, Bandiera E, Pecorelli S (2007) Overexpression of Clostridium perfringens enterotoxin receptors claudin-3 and claudin-4 in uterine carcinosarcomas. Clin Cancer Res 13:3339–3346
14. Maeda T, Murata M, Chiba H, Takasawa A, Tanaka S, Kojima T, Masumori N, Tsukamoto T, Sawada N (2012) Claudin-4-targeted therapy using Clostridium perfringens enterotoxin for prostate cancer. Prostate 72:351–360
15. Morin PJ (2005) Claudin proteins in human cancer: promising new targets for diagnosis and therapy. Cancer Res 65:9603–9606
16. Kominsky SL (2006) Claudins: emerging targets for cancer therapy. Expert Rev Mol Med 8:1–11
17. Goetsch L, Haeuw JF, Bear-Larvor C, Gonzalez A, Zanna L, Malissard M, Lepecquet AM, Robert A, Bailly C, Broussas M, Corvaia N (2012) A novel role for junctional adhesion moleculea-A in tumor proliferation: modulation by an anti-JAM-A monoclonal antibody. Int J Cancer 132:1463–1474
18. Murakami M, Giampietro C, Giannotta M, Corada M, Torselli I, Orsenigo F, Cocito A, d'Ario G, Mazzarol G, Confalonieri S, Di Fiore PP, Dejana E (2011) Abrogation of junctional adhesion molecule-A expression induces cell apoptosis and reduces breast cancer progression. PLoS One 6:e21242
19. El-Naggar AK (2017) Tumors of the salivary glands. In: El-Naggar AK, Chan JKC, Grandis JR, Takata T, Slootweg PJ (eds) World Health Organization Classification of Tumors. WHO classification of head and neck tumours, 4th edn. International Agency for Research on Cancer Press, Lyon, pp 160–202
20. Baker OJ (2010) Tight junctions in salivary epithelium. J Biomed Biotechnol 2010:278948
21. Baker OJ (2016) Current trends in salivary gland tight junctions. Tissue Barriers 4:e1162348
22. Tang VW, Goodenough DA (2003) Paracellular ion channel at the tight junction. Biophys J 84:1660–1673
23. Kriegs JO, Homann V, Kinne-Saffran E, Kinne RK (2007) Identification and subcellular localization of paracellin-1 (claudin-16) in human salivary glands. Histochem Cell Biol 128:45–53
24. Lourenço SV, Coutinho-Camillo CM, Buim ME, Uyekita SH, Soares FA (2007) Human salivary gland branching morphogenesis: morphological localization of claudins and its parallel relation with developmental stages revealed by expression of cytoskeleton and secretion markers. Histochem Cell Biol 128:361–369
25. Maria OM, Kim JW, Gerstenhaber JA, Baum BJ, Tran SD (2008) Distribution of tight junction proteins in adult human salivary glands. J Histochem Cytochem 56:1093–1098
26. Ewert P, Aguilera S, Alliende C, Kwon YJ, Albornoz A, Molina C, Urzúa U, Quest AF, Olea N, Pérez P, Castro I, Barrera MJ, Romo R, Hermoso M, Leyton C, González MJ (2010) Disruption of tight junction structure in salivary glands from Sjögren's syndrome patients is linked to proinflammatory cytokine exposure. Arthritis Rheum 62:1280–1289
27. Mellas RE, Leigh NJ, Nelson JW, McCall AD, Baker OJ (2015) Zonula occludens-1, occludin and E-cadherin expression and organization in salivary glands with Sjögren's Syndrome. J Histochem Cytochem 63:45–56
28. Abe A, Takano K, Kojima T, Nomura K, Kakuki T, Kaneko Y, Yamamoto M, Takahashi H, Himi T (2016) Interferon-gamma increased epithelial barrier function via upregulating claudin-7 expression in human submandibular gland duct epithelium. J Mol Histol 47:353–363
29. Aro K, Rosa LE, Bello IO, Soini Y, Mäkitie AA, Salo T, Leivo I (2011) Expression pattern of claudins 1 and 3—an auxiliary tool in predicting behavior of mucoepidermoid carcinoma of salivary gland origin. Virchows Arch 458:341–348
30. Abd El-Ghani SF, Kasem RF, Ghallab NA, Shaker OG (2013) Detection of claudin-4 in salivary gland neoplasms (a study

utilizing RT-PCR and immunohistochemistry). J Oral Pathol Med 42:781–787
31. Remmele W, Hildebrand U, Hienz HA, Klein PJ, Vierbuchen M, Behnken LJ, Heicke B, Scheidt E (1986) Comparative histological, histochemical, immunohistochemical and biochemical studies on oestrogen receptors, lectin receptors, and Barr bodies in human breast cancer. Virchows Arch A Pathol Anat Histopahtol 409:127–147
32. Keira Y, Takasawa A, Murata M, Nojima M, Takasawa K, Ogino J, Higashiura Y, Sasaki A, Kimura Y, Mizuguchi T, Tanaka S, Hirata K, Sawada N, Hasegawa T (2015) An immunohistochemical marker panel including claudin-18, maspin, and p53 improves diagnostic accuracy of bile duct neoplasms in surgical and presurgical biopsy specimens. Virchows Arch 466:265–277
33. Mi Jeong Kwon (2013) emerging roles of claudins in human cancer. Int J Mol Sci 14:18148–18180
34. Huang J, Zhang L, He C, Qu Y, Li J, Zhang J, Du T, Chen X, Yu Y, Liu B, Zhu Z (2015) Claudin-1 enhances tumor proliferation and metastasis by regulating cell anoikis in gastric cancer. Oncotarget 6:1652–1665
35. Chang TL, Ito K, Ko TK, Liu Q, Salto-Tellez M, Yeoh KG, Fukamachi H, Ito Y (2010) Claudin-1 has tumor suppressive activity and is a direct target of RUNX3 in gastric epithelial cells. Gastroenterology 138:255–265
36. Pope JL, Ahmad R, Bhat AA, Washington MK, Singh AB, Dhawan P (2014) Claudin-1 overexpression in intestinal epithelial cells enhances susceptibility to adenomatous polyposis coli-mediated colon tumorigenesis. Mol Cancer 13:167
37. Bezdekova M, Brychtova S, Sedlakova E, Langova K, Brychta T, Belej K (2012) Analysis of Snail-1, E-cadherin and claudin-1 expression in colorectal adenomas and carcinomas. Int J Mol Sci 13:1632–1643
38. Huo Q, Kinugasa T, Wang L, Huang J, Zhao J, Shibaguchi H, Kuroki M, Tanaka T, Yamashita Y, Nabeshima K, Iwasaki H, Kuroki M (2009) Claudin-1 protein is a major factor involved in the tumorigenesis of colorectal cancer. Anticancer Res 29:851–857
39. Weber CR, Nalle SC, Tretiakova M, Rubin DT, Turner JR (2008) Claudin-1 and claudin-2 expression is elevated in inflammatory bowel disease and may contribute to early neoplastic transformation. Lab Invest 88:1110–1120
40. Tőkés A-M, Kulka J, Paku S, Szik Á, Páska C, Novák PK, Szilák L, Kiss A, Bögi K, Schaff Z (2005) Claudin-1, -3 and – 4 proteins and mRNA expression in benign and malignant breast lesions: a research study. Breast Cancer Res 7:R296–R305
41. Myal Y, Leygue E, Blanchard AA (2010) Claudin 1 in breast tumorigenesis: revelation of a possible novel "claudin high" subset of breast cancers. J Biomed Biotechnol 2010:956897
42. Tokés AM, Kulka J, Paku S, Szik A, Páska C, Novák PK, Szilák L, Kiss A, Bögi K, Schaff Z (2005) Claudin-1, -3 and -4 proteins and mRNA expression in benign and malignant breast lesions: a research study. Breast Cancer Res 7:R296–R305
43. Yoon CH, Kim MJ, Park MJ, Park IC, Hwang SG, An S, Choi YH, Yoon G, Lee SJ (2009) Claudin-1 acts through c-ABl-PKCdelta signaling and has a causal role in the acquisition of invasive capacity in human liver cells. J Biol Chem 285:226–233
44. Suh Y, Yoon CH, Kim RK, Lim EJ, Oh YS, Hwang SG, An S, Yoon G, Gye MC, Yi JM, Kim MJ, Lee SJ (2012) Claudin-1 induces epithelial-mesenchymal transition through activation of the c-Abl-ERK signaling pathway in human liver cells. Oncogene 32:4873–4882
45. Chao YC, Pan SH, Yang SC, Yu SL, Che TF, Lin CW, Tsai MS, Chang GC, Wu CH, Wu YY, Lee YC, Hong TM, Yang PC (2009) Claudin-1 is a metastasis suppressor and correlates with clinical outcome in lung adenocarcinoma. Am J Respir Crit Care Med 179:123–133
46. Tzelepi VN, Tsamandas AC, Vlotinou HD, Vagianos CE, Scopa CD (2008) Tight junctions in thyroid carcinogenesis: diverse expression of claudin-1, claudin-4, claudin-7 and occludin in thyroid neoplasms. Mod Pathol 21:22–30
47. Zwanziger D, Badziong J, Ting S, Moeller LC, Schmid KW, Siebolts U, Wickenhauser C, Dralle H, Fuehrer D (2015) The impact of CLAUDIN-1 on follicular thyroid carcinoma aggressiveness. Endocr Relat Cancer 22:819–830
48. Goetsch L, Haeuw JF, Beau-Larvor C, Gonzalez A, Zanna L, Malissard M, Lepecquet AM, Robert A, Bailly C, Broussas M, Corvaia N (2013) A novel role for junctional adhesion molecule-A in tumor proliferation: modulation by an anti-JAM-A monoclonal antibody. Int J Cancer 132:1463–1474
49. Takasawa A, Murata M, Takasawa K, Ono Y, Osanai M, Tanaka S, Nojima M, Kono T, Hirata K, Kojima T, Sawada N (2016) Nuclear localization of tricellulin promotes the oncogenic property of pancreatic cancer. Sci Rep 6:33582
50. Akimoto T, Takasawa A, Murata M, Kojima Y, Takasawa K, Nojima M, Aoyama T, Hiratsuka Y, Ono Y, Tanaka S, Osanai M, Hasegawa T, Saito T, Sawada N (2016) Analysis of the expression and localization of tight junction transmembrane proteins, claudin-1, -4, -7, occludin and JAM-A, in human cervical adenocarcinoma. Histol Histopathol 31:921–931